



ARTICLE

Brain monoamine vesicular transport disease caused by homozygous *SLC18A2* variants: A study in 42 affected individuals



ARTICLE INFO

Article history:

Received 7 April 2022

Received in revised form

15 September 2022

Accepted 17 September 2022

Available online 31 October 2022

Keywords:

Brain monoamine vesicular transport disease

Dopamine agonist

Dystonia

SLC18A2

VMAT2

ABSTRACT

Purpose: Brain monoamine vesicular transport disease is an infantile-onset movement disorder that mimics cerebral palsy. In 2013, the homozygous *SLC18A2* variant, p.Pro387Leu, was first reported as a cause of this rare disorder, and dopamine agonists were efficient for treating affected individuals from a single large family. To date, only 6 variants have been reported. In this study, we evaluated genotype–phenotype correlations in individuals with biallelic *SLC18A2* variants.

Methods: A total of 42 affected individuals with homozygous *SLC18A2* variant alleles were identified. We evaluated genotype–phenotype correlations and the missense variants in the affected individuals based on the structural modeling of rat VMAT2 encoded by *Slc18a2*, with cytoplasm- and lumen-facing conformations. A *Caenorhabditis elegans* model was created for functional studies.

Results: A total of 19 homozygous *SLC18A2* variants, including 3 recurrent variants, were identified using exome sequencing. The affected individuals typically showed global developmental delay, hypotonia, dystonia, oculogyric crisis, and autonomic nervous system involvement (temperature dysregulation/sweating, hypersalivation, and gastrointestinal dysmotility). Among the 58 affected individuals described to date, 16 (28%) died before the age of 13 years. Of the 17 patients with p.Pro237His, 9 died, whereas all 14 patients with p.Pro387Leu survived. Although a dopamine agonist mildly improved the disease symptoms in 18 of 21 patients (86%), some affected individuals with p.Ile43Phe and p.Pro387Leu showed milder phenotypes and presented prolonged survival even without treatment. The *C. elegans* model showed behavioral abnormalities.

Conclusion: These data expand the phenotypic and genotypic spectra of *SLC18A2*-related disorders.

© 2022 American College of Medical Genetics and Genomics.

Published by Elsevier Inc. All rights reserved.

Introduction

Monoamine neurotransmitter disorders are rare heterogeneous neurologic disorders mostly presenting during early life.^{1,2} Many neurotransmitter disorders resemble the

phenotypes of other neurologic disorders (eg, cerebral palsy and hypoxic ischemic encephalopathy) and are thus sometimes misdiagnosed.³ When dyskinetic movements occur in combination with autonomic dysregulation, there is a possibility of a neurotransmitter disease, and hence, genetic

Ken Saida and Reza Maroofian contributed equally.

Henry Houlden and Naomichi Matsumoto contributed equally.

*Correspondence and requests for materials should be addressed to Naomichi Matsumoto, Department of Human Genetics, Yokohama City University Graduate School of Medicine, 3-9 Fukuura, Kanazawa-ku, Yokohama, 236-0004, Japan. E-mail address: naomat@yokohama-cu.ac.jp

A full list of authors and affiliations appears at the end of the paper.

doi: <https://doi.org/10.1016/j.gim.2022.09.010>

1098-3600/© 2022 American College of Medical Genetics and Genomics. Published by Elsevier Inc. All rights reserved.

diagnosis should be considered. Biallelic loss-of-function (LoF) variants in *SLC6A3* (OMIM 126455), which encodes a dopamine transporter, cause infantile-onset parkinsonism-dystonia 1 (OMIM 613135), known as dopamine transporter deficiency syndrome (DATS), which is the first monoamine transportopathy to be described.^{4,5} Brain VMAT2, encoded by the *SLC18A2* gene (OMIM 193001) facilitates dopamine and serotonin loading into synaptic vesicles for their transport to the cell membrane and the subsequent release.⁶ Biallelic dysfunction of *SLC18A2* causes brain monoamine vesicular transport disease (infantile-onset parkinsonism-dystonia 2; OMIM 618049).⁷

Heterozygous *Slc18a2*-knockout mice express half the amount of VMAT2 in the brain compared with that in the wild-type mice, and homozygous knockout mice do not express VMAT2 and have poor postnatal viability.^{6,8} A homozygous *SLC18A2* variant (c.1160C>T p.Pro387Leu) in human was first identified in a single large consanguineous family, in which, 8 individuals were affected.⁷ Subsequently, a small number of cases with other *SLC18A2* variants were reported.⁹⁻¹² To date, 6 disease-causing variants in *SLC18A2* have been reported in 7 families, involving 16 affected individuals; among them, only 6 cases have been described in detail.^{7,9-14} In addition, after the first report, each study has described only a single pedigree with 1 disease-causing variant, and thus, comprehensive genetic and clinical aspects of the trait remain elusive.

In this study, we evaluated 19 homozygous *SLC18A2* variants affecting 42 individuals in 27 families. Together with functional studies, our data could better elucidate the molecular and phenotypic spectra of the VMAT2 aberration.

Materials and Methods

Genetic and clinical investigations

We enrolled 42 affected individuals who were newly identified with disease-causing homozygous *SLC18A2* variants through exome/genome sequencing, data sharing with international collaborators, and using GeneMatcher.¹⁵ The study was approved by the appropriate Institutional Review Board. Written informed consent to perform genetic studies and publish clinical data, including photographs, was obtained from the parents of all patients. The clinical features of patients were retrospectively investigated.

Genomic DNA was isolated from peripheral blood leukocytes using standard procedures, and exome/genome sequencing was performed on samples from all affected individuals and in some cases, on samples from their parents. The Genome Aggregation Database¹⁶ and the UK Biobank database¹⁷ were used to select rare variants that were either absent or present at extremely low frequencies in public databases. NM_003054.6 was used as the reference coding sequence for the *SLC18A2* gene. The identified disease-causing variants in *SLC18A2* were confirmed using

Sanger sequencing of polymerase chain reaction (PCR) amplicons. The disease causality of variants was evaluated using in silico prediction scores.

Structural analysis based on homology models

Molecular structural analyses of the mutant proteins were performed based on the conceptual translation of the detected *SLC18A2* variants. Homology models of rat brain rVMAT2 in the cytoplasm- and lumen-facing conformations (accession numbers PM0078823 and PM0080553, respectively) were obtained from the Protein Model DataBase.¹⁸ A model structure of human VMAT2, predicted using AlphaFold (AF-Q05940-F1-model_v2.pdb), was obtained from the AlphaFold Protein Structure Database.¹⁹ Structural considerations and figure preparation were performed using PyMOL (Schrodinger, Inc).

SLC18A2 LoF *C. elegans* model

Worm models of genetic diseases are useful for mechanistic studies of disease-related gene function and for drug repurposing screens.^{20,21} The treatments for patients with *SLC18A2* variants present mixed efficacy, and mutations in the *C. elegans* *SLC18A2* homolog *cat-1*²² remain largely uncharacterized. Therefore, we attempted to develop a suitable *C. elegans* model to identify novel candidate treatments in vivo. CRISPR-Cas9 was used to generate a large putative LoF mutant, *cat-1(syb4974)*. Automated quantitative phenotyping was used to evaluate a consistent multidimensional behavioral phenotype of the disease model in comparison with that of the wild-type strain, N2.

Generation of mutant *C. elegans*

The mutant was designed by SunyBiotech using N2 background as a reference. CRISPR guide RNA was designed to target a large deletion (4508 basepairs), starting close to the start codon and excising several exons from the gene to give high confidence of a putative LoF allele. Deletions were confirmed using PCR.

Worm preparation

All strains were cultured on Nematode Growth Medium at 20 °C and fed *Escherichia coli* (OP50) following a standard procedure.²³ For imaging, synchronized populations of young adult worms were cultured by bleaching unsynchronized gravid adults and allowing L1 diapause progeny to develop for 2.5 days at 20 °C (detailed protocol: <https://dx.doi.org/10.17504/protocols.io.2bzgap6>). On the day of imaging, young adults were washed in M9 (detailed protocol: <https://dx.doi.org/10.17504/protocols.io.bfqbjmsn>), transferred onto imaging plates (3 worms/well) using a COPAS 500 Flow Pilot (detailed protocol: <https://dx.doi.org/10.17504/protocols.io.bfqbjmsn>).

[org/10.17504/protocols.io.bfc9jiz6](https://doi.org/10.17504/protocols.io.bfc9jiz6)), and incubated at 20 °C for 3.5 hours. The plates were transferred onto a multi-camera tracker for another 30 minutes for habituation before imaging (detailed protocol: <https://dx.doi.org/10.17504/protocols.io.bsicncaw>).

Image acquisition, processing, and feature extraction

Videos were acquired and processed following previously described methods.²⁴ In brief, videos were acquired in a room with a nominal temperature of 20 °C at 25 frames per second at a resolution of 12.4 μm per pixel. Three videos were recorded sequentially: a 5-minute prestimulus recording; a 6-minute blue-light recording with three 10-second blue-light pulses starting at 60, 160, and 260 seconds; and a 5-minute poststimulus recording.

The videos were segmented and tracked using Tierpsy Tracker.²⁵ After segmentation and skeletonization, a manual threshold was applied to filter skeletonized objects—likely to be nonworms from feature extraction—that did not meet the following criteria: 200 to 2000 μm in length and 20 to 500 μm in width. In addition, the Tierpsy Tracker viewer was used to mark wells with visible contamination, agar damage, or excess liquid as “bad,” and these wells were excluded from further analysis.

After tracking, we extracted a predefined set of 3076 behavioral features for each well in each of the 3 videos (prestimulus, blue light, and poststimulus).²⁶ The extraction of behavioral features was performed on a per-track basis, and the features were then averaged across tracks to produce a single feature vector for each well. Significant differences between the prestimulus, poststimulus, and blue-light behavioral feature sets extracted from the LoF mutants compared with the N2 reference strain were calculated using block permutation *t* tests (https://github.com/Tierpsy/tierpsy-tools-python/blob/master/tierpsytools/analysis/statistical_tests.py). Python (version 3.8.5) was used to perform the analysis using $n = 1,000,000$ permutations that were randomly shuffled within, but not between, the independent days of image acquisition to control for daily variations in the experiments. The *P* values were then corrected for multiple comparisons using the Benjamini–Hochberg procedure²⁷ to control the false discovery rate at 5%.

Pharyngeal pumping assay

Pharyngeal pumps per minute of the *C. elegans* strains were determined by counting grinder movements by eye over a 20-second period using a stereomicroscope (detailed protocol: <https://doi.org/10.17504/protocols.io.b3hijq4e>) ($n = 120$ worms). Grinder movements of a single worm were counted 3 times, and the results were recorded as an average of these values. Significant differences in pumps per minute between the N2 reference strain and *cat-1* (*syb4974*)

mutants were calculated using block permutation *t* tests with $n = 10,000$ permutations.

Results

Genetic and clinical findings in the affected individuals

Four nonsense variants, 5 frameshift variants, 1 splice site variant, and 9 missense variants (all homozygous) were identified in *SLC18A2* in 27 unrelated families involving 42 affected individuals (Figure 1A). Homozygous variants simply facilitated the establishment of genotype–phenotype correlations. Of the variants identified, 17 were novel, whereas 2 missense variants (NM_003054.6: c.710C>A p.Pro237His and c.1160C>T p.Pro387Leu) were recurrent, accounting for 43% of the cases ($n = 18/42$) described in this article. The most common recurrent missense variant, p.Pro237His, was identified in 12 affected individuals from 6 families. This variant had previously been identified in 5 patients from 3 families.^{9–11} The second most common variant in this cohort was p.Pro387Leu, which was identified in 6 affected individuals from 3 families and has also been previously described in different ethnicities. The novel nonsense variant p.Tyr81 was identified in 3 affected individuals from 2 unrelated families. All predicted disease-causing *SLC18A2* variants identified in this study were either ultrarare or absent in multiple population variant databases (Supplemental Table 1); however, p.Pro237His was relatively frequent in the general population and was found in 6 of 251,386 alleles (0.000024) in Genome Aggregation Database and 35 of 537,496 alleles (0.000065) in the UK Biobank database in heterozygous state.^{16,17} All nonsense and frameshift variants were expected to result in nonsense-mediated messenger RNA decay. All missense variants had Phred-scaled Combined Annotation Dependent Depletion scores of >25 (Supplemental Table 1). Two individuals had other candidate variants; patient 41 with the homozygous *SLC18A2* variant (c.876_883del p.Tyr293Hisfs*43) was described previously²⁸ and had potentially multiple molecular diagnoses owing to compound heterozygous *DDX47* variants (c.[22G>T];[319G>G] p.[p.Asp8Phe]; [p.Gln107Glu]) and a homozygous *SLC13A5* variant (c.1444A>G p.Thr482Ala). Patient 39 with the homozygous *SLC18A2* variant (c.282delA p.Asp95Thrfs*2) had another candidate variant in the *TORIA* gene (c.836T>C p.Met279Thr).

Of the 58 individuals described to date (42 individuals in this study and 16 individuals who were previously reported, with homozygous variants), 16 (28 %) died during childhood (age range: 9 months to 13 years; median: 5.5 years) because of pulmonary complications, sudden cardiorespiratory arrest, or high fever with/without seizures. The clinical features of patients with biallelic disease-causing

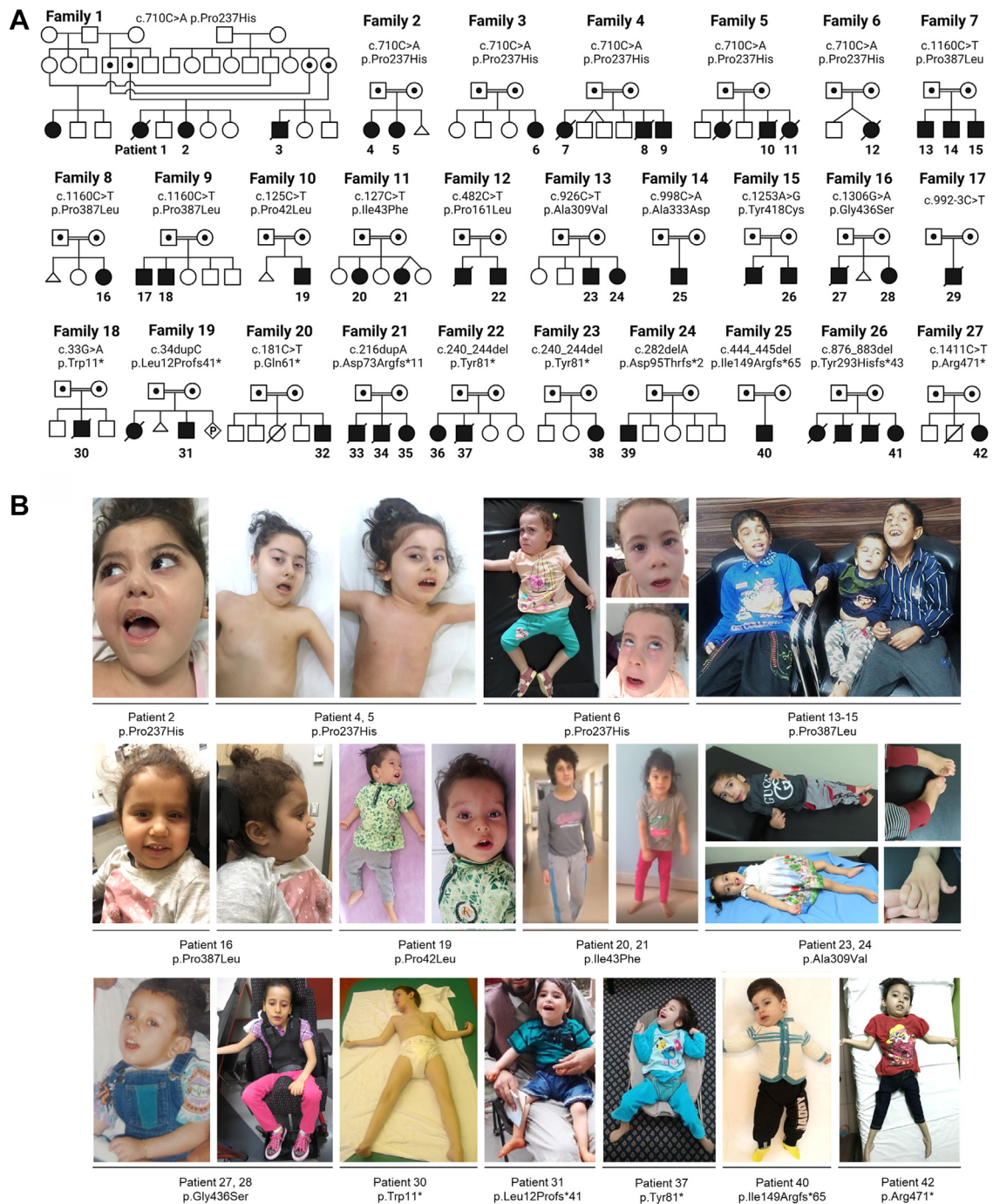


Figure 1 Pedigrees and photographs of individuals with homozygous *SLC18A2* disease-causing variants. A. Family pedigrees of 27 families consisting of 42 affected individuals with homozygous *SLC18A2* variants. B. Clinical photographs of patients 2, 4 to 6, 13 to 16, 19 to 21, 23, 24, 27, 28, 30, 31, 37, 40, and 42.

SLC18A2 variants detected in the previous studies and this study are summarized in [Table 1](#) and fully described in [Supplemental Table 2](#). Except patient 5, who was prematurely born with a birthweight of 1.3 kg, most affected individuals were neurologically normal at birth with no perinatal problems. A few weeks to a few months after birth, the affected individuals began to manifest muscular hypotonia, feeding difficulties, and global developmental delay.

Most individuals presented global developmental delay (100%, 57/57), truncal hypotonia (96%, 53/55), dystonia (94%, 51/54), and parkinsonism (73%, 36/49); however, the severity varied. Oculogyric crisis is a critical sign of this genetic disorder (88%, 44/50). Temperature instability or excessive sweating was observed in 71% (32/45) of the patients. Gastrointestinal problems including dysphagia, hypersalivation, and constipation were frequently observed

Table 1 Overview of core clinical phenotypes of all patients (current and previously reported) with disease-causing homozygous *SLC18A2* variants

Summary		Missense Variants			Truncating and	Total
		Recurrent Variant p.Pro237His	Recurrent Variant p.Pro387Leu	Other Missense Variants	Splice Site Variants	
Demographic	Number of patients	<i>n</i> (<i>N</i> = 17)	<i>n</i> (<i>N</i> = 14)	<i>n</i> (<i>N</i> = 11)	<i>n</i> (<i>N</i> = 15)	<i>n</i> (<i>N</i> = 57) ^a
	Sex (male/female)	8/9	10/4	6/5	8/7	32/25
	Mortality (living status)	53% (8 living/9 dead)	0% (14 living/0 dead)	18% (9 living/2 dead)	33% (10 living/5 dead)	28% (41 living/16 dead)
	Age, median (range), y	5.0 (0.5-14)	11.0 (3-18)	6.3 (1-25)	6.0 (2-16)	5.5 (0.5-25)
Clinical features	GDD/ID	17/17	14/14	11/11	15/15	100% (57/57)
	Truncal hypotonia	17/17	14/14	9/11	13/13	96% (53/55)
	Dystonia	16/16	12/14	10/10	13/14	94% (51/54)
	Parkinsonism	12/16	11/14	6/9	7/10	73% (36/49)
	Nonverbal	13/15	4/7	7/9	9/10	80% (33/41)
	Oculogyric crises	12/12	12/14	9/10	12/14	88% (44/50)
	Epilepsy/seizures	7/12	2/11	5/10	4/12	40% (18/45)
	Other paroxysmal movements	8/14	9/11	4/10	7/13	58% (28/48)
	Temperature instability/sweating	10/12	8/14	6/8	8/11	71% (32/45)
	Feeding issues (dysphagia/NG tube/ gastrostomy)	8/14	3/7	6/10	10/12	63% (32/43)
	Hypersalivation (drooling)	10/11	12/14	5/9	8/11	78% (35/45)
	Constipation	3/4	1/2	5/7	9/12	69% (18/26)
Imaging findings	Normal findings	8/15	2/5	3/7	2/10	40% (15/37)
	Corpus callosum hypoplasia	1/15	0/5	1/7	3/10	14% (5/37)
	Nonspecific WM abnormalities	2/15	2/5	1/7	5/10	27% (10/37)
	Brain atrophy	4/15	1/5	2/7	4/10	30% (11/37)
Treatment	L-DOPA use	3/18	4/14	8/11	5/14	35% (20/57)
	Deterioration on L-DOPA	3/3	4/4	2/8	3/5	60% (12/20)
	Dopamine agonist use	3/18	5/14	7/11	6/14	37% (21/57)
	Improvement on dopamine agonist	3/3	5/5	6/7	4/6	86% (18/21)

GDD, global developmental delay; *ID*, intellectual disability; *L-DOPA*, levodopa; *NG*, nasogastric; *WM*, white matter.

^aA patient with compound heterozygous variants (c.[895G>C];[835_836delAG] p.[Gly299Arg];[Gln280Glufs*58]) (PMID: 31618753) was excluded from [Table 1](#) because of a lack of detailed clinical information.

in 63% (32/43), 78% (35/45), and 69% (18/26) of the patients, respectively, and several patients required supplemental nasogastric feeding or gastrostomy. Epilepsy or seizures occurred in 40% (18/45) and other paroxysmal movements were observed in 58% (28/48) of the patients. Nonetheless, the electroencephalograms were normal or at least did not correlate well with seizures or other paroxysmal movements. Several patients showed intention tremor or ataxia, although, we could not obtain sufficient information for most patients.

The brain images were typically normal (40%, 15/37), although, subtle changes were occasionally observed (eg, cerebral atrophy/cortical volume loss/mild ventricle enlargement in 30% [11/37], nonspecific white matter abnormalities in 27% [10/37], corpus callosum hypoplasia in 14% [5/37] of the patients; [Table 1](#); [Supplemental Figure 1](#)). Cerebrospinal fluid (CSF) neurotransmitter analysis was performed in 4 patients, and homovanillic acid (HVA) and 5-hydroxyindoleacetic acid (5-HIAA) levels were within normal limits ([Supplemental Table 3](#)).

In total, 80% (33/41) of the patients were nonverbal and most of them were nonambulatory. 14 affected individuals with nonsense, frameshift, and splice site variants were mostly nonverbal, in a bed-bound state, and had more severe symptoms than those with missense variants (eg, [Figure 1B](#); photographs of patients 30, 31, 34, 40, and 42 with truncating variants). Notably, differences in disease severity were observed among the affected individuals with missense variants, wherein the patients with p.Pro237His showed severe phenotypes similar to those with null variants, whereas some with p.Ile43Phe or p.Pro387Leu variants were ambulatory and verbal. Patients 20 and 21, both harboring homozygous p.Ile43Phe variants, started to walk at the age of 3 and 2.5 years, respectively, and speak short sentences at the age of 4 and 3 years, respectively. ([Figure 1B](#); [Supplemental Videos 1-3](#)). Videos of other patients' activity are available for patients 2, 13-15, 26, 30, 36, and 37 ([Supplemental Videos 4-9](#)).

Levodopa treatment was either ineffective or had an adverse effect, whereas dopamine agonist treatment (eg, pramipexole and bromocriptine) mildly improved symptoms in 86% (18/21) of the patients ([Table 1](#), [Supplemental Table 2](#)). Specifically, pramipexole at 0.01 to 0.02 mg/kg/day divided into 1 to 3 doses was initiated; if a patient tolerated this dose without adverse effects, it was increased.²⁹ Symptom improvement was observed in alertness, parkinsonism, dystonia, and oculogyric crisis, although, it varied with each patient. The increased dose of pramipexole caused agitation or nausea in a few cases.

Mapping of disease-causing *SLC18A2* missense variants on the VMAT2 structural models

The structure of human VMAT2 has not been experimentally determined. However, homology models of the rat protein (rVMAT2) have been constructed using related

transporter structures as templates to represent 3 conformational states in the transport cycle (cytoplasm-facing, occluded, and lumen-facing conformations).^{30,31} These models agree well with a model created by an artificial intelligence-based structure prediction program, AlphaFold2, in terms of distribution of transmembrane helices.¹⁴

We mapped the positions of missense variants on the structural models of rVMAT2. The models contain 2 domains (the N- and C-domains), each consisting of 6 transmembrane helices,³² and their relative orientation changes between the cytoplasm- and lumen-facing conformations ([Figure 2](#)). Proline and glycine residues—generally known as helix breakers—occur at multiple transmembrane helices and are assumed to facilitate the conformational distortion or flexibility of VMAT2; this is essential for proton-coupled conformational changes in the transport cycle.³² Notably, among the 9 variants reported in this study, 4 affect prolines (p.Pro42Leu, p.Pro161Arg, p.Pro237His, and p.Pro387Leu) and 1 affects glycine (p.Gly436Ser) in the transmembrane helices. These variants could perturb the conformational dynamics and subsequently, the transport activity of VMAT2.

Specifically, rVMAT2 carrying the p.Pro42Leu substitution (equivalent to human VMAT2 p.Pro42Leu) abolishes serotonin transport activity.³³ In the cytoplasm-facing conformation, Pro42 and the adjacent Ile43 are located at the bottom of the central cavity, which accommodates the monoamine substrates ([Figure 2B](#)). Pro42 and Ile43 are positioned at the bend of transmembrane helix 1 (TM1) in the cytoplasm-facing conformation ([Figure 2D](#)); TM1 is stretched in the lumen-facing conformation ([Figure 2C](#) and [E](#)). Therefore, the p.Pro42Leu and p.Ile43Phe substitutions may affect this conformational transition of TM1, leading to decreased monoamine transport activity.

Similar to Pro42, Ala310 of rVMAT2 (equivalent to human VMAT2 Ala309) faces the central cavity in the cytoplasm-facing conformation ([Figure 2D](#)). It is located on TM7 and is 1 turn away from Glu313, an essential residue for monoamine transport activity. Glu313 directly binds to the monoamines and/or protons; therefore, the human p.Ala309Val substitution may affect the transportation. In rVMAT2, Tyr419 (equivalent to human Tyr418) has been proposed to constitute a part of the cytoplasmic gate. The rVMAT2 variants carrying p.Tyr419Ser and p.Tyr419Ala, but not p.Tyr419Phe, lack serotonin transport activities.³¹ Therefore, a human VMAT2 variant carrying p.Tyr418-Cys, without an aromatic ring, may exhibit impaired transport activity.

C. elegans model mimicking LoF abnormalities in *SLC18A2*

To create a *C. elegans* disease model, we deleted *cat-1*, the worm homolog of *SLC18A2*. The mutant showed increased curvature of the head and neck and slow movement and was generally more stationary than the wild-type reference strain

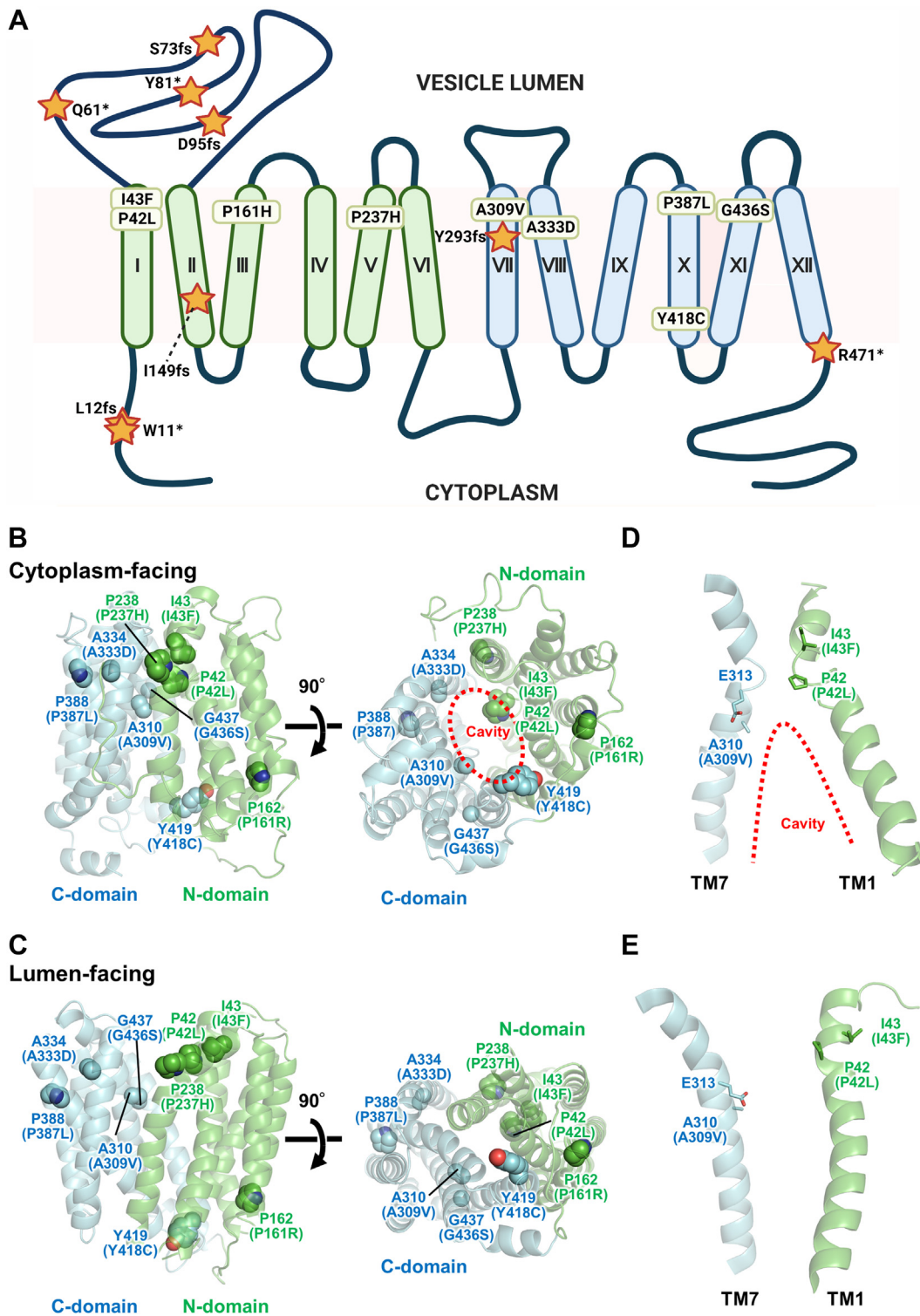


Figure 2 Disease-causing *SLC18A2* variants and protein structures. (A) Location of 9 missense, 4 nonsense, and 5 frameshift *SLC18A2* disease-causing variants found in this study. (B-E) 3 dimension protein structures. The positions of the disease-causing variants are mapped onto the homology models of rVMAT2. The N- and C-domains are colored green and cyan, respectively. The rat residues and corresponding human disease-causing variants (in parentheses) are indicated. The central cavity, which accommodates substrates in the cytoplasm-facing conformation, is indicated using a red dotted line. B, C. Cytoplasm-facing (B) and lumen-facing (C) conformations. Left, side view. Right, top view from the cytoplasm. D, E. The structures of transmembrane helix 1 (TM1) and TM7 in the cytoplasm-facing (D) and lumen-facing (E) conformations.

N2 (Supplemental Figure 2A-D). Upon stimulation with an aversive stimulus (pulses of blue light), *cat-1(syb4974)* mutant showed a hypersensitive, but short-lived, photophobic escape response (Supplemental Figure 2F-I). We noted that the *cat-1(syb4974)* mutant phenotype closely resembled that of another *C. elegans* model of hypotonia, *nca-2(syb1612)* mutant, which has a LoF variant in the sodium cation leak channel (unpublished data). Therefore, *C. elegans* exhibits a conserved multidimensional behavioral phenotype on the basis of the variants in different genes; the symptoms overlap with those in humans with the corresponding variant. The observed behavioral phenotypes are noticeable in short recordings with reasonable throughput,²⁴ making them an appropriate readout for drug repurposing screens similar to others that have been successful in recording *C. elegans* using whole-organism phenotypes.^{20,21}

Effects of monoamine on the *C. elegans* model

Consistent with previous reports on the effects of VMAT variants on monoamine-dependent behaviors in *C. elegans*,³⁴ the *cat-1(syb4974)* mutant exhibited a decreased pharyngeal pumping rate when foraging on a bacterial lawn (Supplemental Figure 2E). Based on previous studies on the treatment of monoamine disturbances in humans, we exposed the *cat-1(syb4974)* mutant worms to carbidopa, dopamine, levodopa, or pramipexole for 4 hours. No significant changes were observed in the phenotypes of any *cat-1(syb4974)* mutant worms at any of the concentrations (0.1-500 μ M) compared with control worms (exposed to the solvent only) (Supplemental Figure 3). The lack of significant modulation by the compounds that we tested may be due to a lack of drug accumulation in the worms³⁵ and, therefore, longer treatments at higher concentrations should be considered in future studies.

Discussion

In this article, we described the clinical manifestations observed in 42 individuals from 27 families of different ethnicities with 17 novel and 2 previously reported *SLC18A2* variants. Among the affected individuals in this and previous studies, p.Pro237His is the most common disease-causing variant. This variant is found relatively frequently across multiple variant databases and could be an ancient founder variant. The high mortality rate indicates the poor prognosis of this genetic disorder. Notably, 9 of the 17 patients with p.Pro237His (median age: 5.0 [0.5-14] years) died, whereas all 14 patients with p.Pro387Leu (median age: 11.0 [3-18] years) survived. In addition, although the affected individuals with homozygous *SLC18A2* variants were often in bed-bound states, those with p.Ile43Phe and p.Pro387Leu were able to walk, indicating a mild clinical phenotype. In contrast, the affected individuals with p.Pro237His exhibited

a severe phenotype and poor prognosis, similar to those of individuals with truncating variants. Consistent with this observation, Jacobsen et al⁹ reported that patients with p.Pro237His showed a more severe phenotype than the affected individuals with p.Pro387Leu. These observations indicate a phenotype-genotype correlation in *SLC18A2*-related disorder.

Affected individuals with *SLC18A2* variants showed global developmental delay, hypotonia, dystonia, parkinsonism, and autonomic nervous system involvement (eg, temperature dysregulation/sweating, hypersalivation, gastrointestinal dysmotility, and oculogyric dysmotility). Autonomic dysregulation in combination with extrapyramidal movements, in the presence of structurally normal basal ganglia, is an important clinical feature to distinguish cerebral palsy from this neurotransmitter disease. Other neurotransmitter disorders such as *SLC6A3*-related DATS and aromatic l-amino acid decarboxylase deficiency (OMIM 608643)³⁶ are possible differential diagnoses, and CSF neurotransmitter analysis is an essential diagnostic tests. Typically, *SLC6A3*-related DATS have a high HVA with a normal 5-HIAA ratio (CSF HVA/5-HIAA ratio >5), whereas aromatic l-amino acid decarboxylase deficiency has low levels of both HVA and 5-HIAA.^{5,36} In contrast, both HVA and 5-HIAA levels in the CSF were within the normal limits in this study, which is consistent with previous reports on *SLC18A2*-related disorder.^{7,9,12} These observations are key findings to differentiate this genetic disorder from other neurotransmitter disorders.

Both p.Pro237His and p.Pro387Leu variants affect proline residues located on transmembrane helices (Figure 2A and B), and patients with p.Pro237His have severe phenotypes. In the cytoplasm- and lumen-facing conformation of rVMAT2 (Figure 2C and E), Pro238 (equivalent to human VMAT2 Pro237) is located at the interface between the N- and C-domains, presumably forming a part of the hinge region in the conformation of the 2 domains. Therefore, the Pro237His substitution in human VMAT2 could also affect the conformations of the 2 domains during the transport cycle. Alternatively, the Pro237His variant could be energetically unstable because of the relatively hydrophilic Pro237His side-chain embedded in the lipid bilayer.

VMAT2 is well established as a therapeutic target.^{29,37} Levodopa is either ineffective or worsens the symptoms in patients, whereas dopamine agonists improve the symptoms. The treatment efficacy was difficult to assess because of the short treatment periods; a mild symptom improvement was observed in 86% of the patients treated with a dopamine agonist. This finding might be inconsistent with the earliest report describing a dramatic therapeutic effect of a dopamine agonist in a large family of patients with p.Pro387Leu variants.⁷ p.Pro387Leu causes a relatively mild phenotype, and drug responses should be cautiously evaluated alongside phenotype-genotype correlation.⁹ Patients 20 and 21 from family 11 (with p.Ile43Phe) were able to walk and speak, even without treatment; therefore, certain genetic variants may have a higher effect on illness severity than the treatment itself.

A *C. elegans* model was constructed to mimic the affected individuals with LoF variants; it exhibited slow movement, a hypersensitive but short-lived photophobic escape response, and a decreased pharyngeal pumping rate. Therefore, the *SLC18A2* LoF could be harmful, at least in worms and humans. We did not observe any rescue of *cat-1* mutant phenotypes in response to dopamine or dopamine agonists at the tested concentrations.

The solute carrier (SLC) protein family is a superfamily of transmembrane transporters with >400 members that are involved in the exchange of amino acids, nutrients, ions, metals, neurotransmitters, and metabolites across various biological membranes.³⁸ To date, 287 SLC genes have been found in the brain, and variants or dysfunctions of >70 SLC-encoding genes have been shown to be associated with a variety of human brain disorders, such as severe developmental delay or epileptic encephalopathies.³⁹⁻⁴²

In summary, in combination with previously published data, we identified the genetic and clinical features of 42 newly affected individuals with homozygous *SLC18A2* variants. We elucidated the clinical synopsis of the trait together with functional study results. These findings may facilitate the establishment of genotype–phenotype correlations for *SLC18A2*-associated parkinsonism-dystonia syndrome. This allelic series study provides initial insights into *SLC18A2*-related disorders with both diagnostic and therapeutic implications.

Data Availability

The data sets of this study are not publicly available owing to concerns regarding patients' anonymity. We will supply de-identified data upon request.

Acknowledgments

We thank the participants and their families for their involvement in this study. This work was supported by the Japan Agency for Medical Research and Development (AMED) under grant numbers JP22ek0109486, JP22ek0109549, and JP22ek0109493 (N.Ma.); Japan Society for the Promotion of Science (JSPS) KAKENHI under grant numbers JP19H03621 (N.Mi.), JP20K07907 (S.M.), JP20K08164 (T.Miz.), JP20K17936 (A.F.), JP20K16932 (K.H.), and JP21k15907 (Y.U.); and the Takeda Science Foundation (T.Miz., N.Mi., and N.Ma.). This study was partially supported by the US National Human Genome Research Institute and National Heart Lung and Blood Institute to the Baylor-Hopkins Center for Mendelian Genomics (UM1 HG006542 to J.R.L.), US National Institute of Neurological Disorders and Stroke (R35NS105078 to J.R.L.), and Muscular Dystrophy Association (512848 to J.R.L.). D.Ma. was supported by a Medical Genetics Research Fellowship Program through the National

Institutes of Health (T32 GM007526-42). D.P. was supported by a Clinical Research Training Scholarship in Neuromuscular Disease partnered by the American Academy of Neurology, American Brain Foundation, and Muscle Study Group and by the International Rett Syndrome Foundation (grant number #3701-1). J.E.P. was supported by the National Human Genome Research Institute (K08 HG008986). H.H. was funded by the Medical Research Council (MRC) (MR/S01165X/1, MR/S005021/1, and G0601943), NIHR University College London Hospitals Biomedical Research Centre, Rosetree Trust, Ataxia UK, Multiple System Atrophy Trust, Brain Research UK, Sparks Great Ormond Street Hospital Charity, Muscular Dystrophy UK, and Muscular Dystrophy Association. N.D. was supported by an MRC strategic award to establish International Centre for Genomic Medicine in Neuromuscular Diseases (MR/S005021/1). This project also received funding from the European Research Council under the European Union's Horizon 2020 Research and Innovation Program (grant agreement number 714853) and was supported by the Medical Research Council through grant MC-A658-5TY30. We acknowledge the support of King Salman Center for Disability Research through Research Group no RG-2022-010 (F.S.A.). Figure 1A, 2A, and Graphical Abstract were created with BioRender.com.

Author Information

K.Sai. and R.M. conceived and designed the study, interpreted the data, and wrote the manuscript. T.S. and K.O. conducted protein structure analysis and wrote the manuscript. T.J.O. and E.G.K. performed the *C. elegans* experiments. T.Mit., M.T., H.Y.L., G.A., H.G., M.Z., M.B.T., F.As., S.I., H.M., N.A., V.K.G., V.M.S., D.Ma., R.K., N.D., H.T., H.M.E., K.R., S.Y., S.K., M.H., M.P., D.A., J.R.M.C., C.A.K., K.G.M., K.G.L., H.Y., M.S.Z., R.M.E., K.Sal., U.G., M.M., S.S., and M.A. recruited the patients and performed the clinical evaluation. D.P., M.Se., M.Sr., D.B., S.Als., S.Ala., S.A.M.M., H.A., M.A.-O., L.A., F.Ab., T.J., R.E.G., H.S., D.K., T.S.R., F.S., D.Mi., and B.A. helped obtain clinical information on the patients reported in this study. A.T.P., Y.B., A.M., G.Y., E.S., S.G., and D.P. contributed to genetic data analysis. S.O., K.H., A.F., Y.U., T.Miz., S.M., E.F., D.Mu., R.R., and C.J.C. conducted DNA sequencing and genetic data analysis. P.S., A.G., F.S.A., A.E.X.B., and J.E.P. evaluated the data and wrote the manuscript. N.Mi., J.G.G., J.R.L., H.H., and N.Ma. conducted and supervised this study, wrote the manuscript, and secured funding.

Ethics Declaration

Written informed consent for publication was obtained from the parents of each patient. Ethics approval for this study

was obtained from the Institutional Review Board of Yokohama City University School of Medicine, Baylor College of Medicine, University College London, the Norwegian South-Eastern Regional Ethics Committee, and each genetic analysis center.

Conflict of Interest

K.G.M., K.G.L., and H.Y. are employees of GeneDx, Inc. J.R.L. has stock ownership in 23andMe, is a paid consultant for Regeneron Pharmaceuticals, and is a coinventor on multiple United States and European patents related to molecular diagnostics for inherited neuropathies, eye diseases, genomic disorders, and bacterial genomic fingerprinting. The Department of Molecular and Human Genetics at Baylor College of Medicine receives revenue from clinical genetic testing conducted at Baylor Genetics Laboratories. All other authors declare no conflicts of interest.

Additional Information

The online version of this article (<https://doi.org/10.1016/j.gim.2022.09.010>) contains supplementary material, which is available to authorized users.

Authors

Ken Saida¹ , Reza Maroofian², Toru Sengoku³, Tadahiro Mitani⁴, Alistair T. Pagnamenta⁵, Dana Marafi^{4,6}, Maha S. Zaki⁷, Thomas J. O'Brien^{8,9}, Ehsan Ghayoor Karimiani^{10,11}, Rauan Kaiyrzhanov², Marina Takizawa¹, Sachiko Ohori¹, Huey Yin Leong¹², Gulsen Akay⁴, Hamid Galehdari¹³, Mina Zamani¹³, Ratna Romy¹⁰, Christopher J. Carroll¹⁰, Mehran Beiraghi Toosi^{14,15}, Farah Ashrafzadeh¹⁴, Shima Imannezhad¹⁶, Hadis Malek¹⁷, Najmeh Ahangari¹⁷, Hoda Tomoum¹⁸, Vykuntaraju K. Gowda¹⁹, Varunvenkat M. Srinivasan¹⁹, David Murphy²⁰, Natalia Dominik², Hasnaa M. Elbendary⁷, Karima Rafat⁷, Sanem Yilmaz²¹, Seda Kanmaz²¹, Mine Serin²¹, Deepa Krishnakumar²², Alice Gardham²², Anna Maw²³, Tekki Sreenivasa Rao²⁴, Sarah Alsubhi²⁵, Myriam Srour^{25,26}, Daniela Buhas^{27,28}, Tamison Jewett²⁹, Rachel E. Goldberg²⁹, Hanan Shamseldin³⁰, Eirik Frengen³¹, Doriana Misceo³¹, Petter Strømme³², José Ricardo Magliocco Ceroni³³, Chong Ae Kim³³, Gozde Yesil³⁴, Esmâ Sengenc³⁵, Serhat Guler³⁶, Mariam Hull³⁷, Meredith Parnes³⁷, Dilek Aktas³⁸, Banu Anlar³⁹, Yavuz Bayram^{40,41}, Davut Pehlivan^{4,37,42}, Jennifer E. Posey⁴, Shahryar Alavi⁴³, Seyed Ali Madani Manshadi⁴⁴, Hamad Alzaidan⁴⁵, Mohammad Al-Owain⁴⁵, Lama Alabdi^{30,46},

Ferdous Abdulwahab³⁰, Futoshi Sekiguchi¹, Kohei Hamanaka¹, Atsushi Fujita¹, Yuri Uchiyama^{1,47}, Takeshi Mizuguchi¹, Satoko Miyatake^{1,48}, Noriko Miyake^{1,49}, Reem M. Elshafie⁵⁰, Kamran Salayev⁵¹, Ulviyya Guliyeva⁵², Fowzan S. Alkuraya^{30,53}, Joseph G. Gleeson^{54,55}, Kristin G. Monaghan⁵⁶, Katherine G. Langley⁵⁶, Hui Yang⁵⁶, Mahsa Motavaf⁵⁷, Saeid Safari⁵⁷, Mozghan Alipour^{57,58}, Kazuhiro Ogata³, André E.X. Brown^{8,9}, James R. Lupski^{4,37,59,60}, Henry Houlden², Naomichi Matsumoto^{1,*} 

Affiliations

¹Department of Human Genetics, Yokohama City University Graduate School of Medicine, Yokohama, Japan; ²Department of Neuromuscular Disorders, UCL Queen Square Institute of Neurology, University College London, London, United Kingdom; ³Department of Biochemistry, Yokohama City University Graduate School of Medicine, Yokohama, Japan; ⁴Department of Molecular and Human Genetics, Baylor College of Medicine, Houston, TX; ⁵NIHR Oxford Biomedical Research Centre, Wellcome Centre for Human Genetics, University of Oxford, Oxford, United Kingdom; ⁶Department of Pediatrics, Faculty of Medicine, Kuwait University, Safat, Kuwait; ⁷Department of Clinical Genetics, Human Genetics and Genome Research Institute, National Research Centre, Cairo, Egypt; ⁸MRC London Institute of Medical Sciences, London, United Kingdom; ⁹Faculty of Medicine, Institute of Clinical Sciences, Imperial College London, London, United Kingdom; ¹⁰Molecular and Clinical Sciences Research Institute, St. George's, University of London, London, United Kingdom; ¹¹Innovative Medical Research Center, Mashhad Branch, Islamic Azad University, Mashhad, Iran; ¹²Genetics Department, Hospital Kuala Lumpur, Kuala Lumpur, Malaysia; ¹³Department of Biology, Faculty of Science, Shahid Chamran University of Ahvaz, Ahvaz, Iran; ¹⁴Department of Pediatrics, Faculty of Medicine, Mashhad University of Medical Sciences, Mashhad, Iran; ¹⁵Neuroscience Research Center, Mashhad University of Medical Sciences, Mashhad, Iran; ¹⁶Department of Pediatric Neurology, Faculty of Medicine, Mashhad University of Medical Sciences, Mashhad, Iran; ¹⁷Department of Medical Genetics, Next Generation Genetic Polyclinic, Mashhad, Iran; ¹⁸Department of Pediatrics, Ain Shams University, Cairo, Egypt; ¹⁹Department of Pediatric Neurology, Indira Gandhi Institute of Child Health, Bangalore, India; ²⁰Department of Clinical and Movement Neurosciences, UCL Queen Square Institute of Neurology, University College London, London, United Kingdom; ²¹Division of Pediatric Neurology, Department of Pediatrics, Ege University Faculty of Medicine, Izmir, Turkey; ²²North West Thames Regional Genetics Service, Northwick Park Hospital, London, United Kingdom; ²³Department of Paediatric Neurology, Cambridge University Hospitals NHS Foundation Trust,

Cambridge, United Kingdom; ²⁴Department of Paediatrics, Luton and Dunstable University Hospital, Luton, United Kingdom; ²⁵Division of Pediatric Neurology, Departments of Pediatrics, McGill University, Montreal, Quebec, Canada; ²⁶Research Institute of the McGill University Health Center (MUHC), Montreal, Quebec, Canada; ²⁷Division of Medical Genetics, Department of Specialized Medicine, McGill University Health Center (MUHC), Montreal, Quebec, Canada; ²⁸Department of Human Genetics, McGill University, Montreal, Quebec, Canada; ²⁹Department of Pediatrics, Section on Medical Genetics, Wake Forest University School of Medicine, Winston-Salem, NC; ³⁰Department of Translational Genomics, Center for Genomic Medicine, King Faisal Specialist Hospital and Research Center, Riyadh, Saudi Arabia; ³¹Department of Medical Genetics, Oslo University Hospital and University of Oslo, Oslo, Norway; ³²Division of Pediatric and Adolescent Medicine, Oslo University Hospital and University of Oslo, Oslo, Norway; ³³Genetic Unit, Instituto da Crianca, Faculdade de Medicina, Universidade de Sao Paulo, Sao Paulo, Brazil; ³⁴Department of Medical Genetics, Istanbul Faculty of Medicine, Istanbul University, Istanbul, Turkey; ³⁵Department of Pediatric Neurology, Faculty of Medicine, Bezmialem Vakif University, Istanbul, Turkey; ³⁶Department of Child Neurology, Cerrahpasa Medical Faculty, Istanbul University, Istanbul, Turkey; ³⁷Texas Children's Hospital, Houston, TX; ³⁸Damagen Genetic Diagnostic Center, Ankara, Turkey; ³⁹Department of Pediatric Neurology, Hacettepe University Faculty of Medicine, Ankara, Turkey; ⁴⁰Division of Genomic Diagnostics, Department of Pathology and Laboratory Medicine, Children's Hospital of Philadelphia, Philadelphia, PA; ⁴¹Perelman School of Medicine, University of Pennsylvania, Philadelphia, PA; ⁴²Division of Pediatric Neurology and Developmental Neuroscience, Department of Pediatrics, Baylor College of Medicine, Houston, TX; ⁴³Department of Cell and Molecular Biology and Microbiology, Faculty of Biological Science and Technology, University of Isfahan, Isfahan, Iran; ⁴⁴Meybod Genetic Research Center, Meybod, Yazd, Iran; ⁴⁵Department of Medical Genetics, King Faisal Specialist Hospital and Research Center, Riyadh, Saudi Arabia; ⁴⁶Department of Zoology, College of Science, King Saud University, Riyadh, Saudi Arabia; ⁴⁷Department of Rare Disease Genomics, Yokohama City University Hospital, Yokohama, Japan; ⁴⁸Clinical Genetics Department, Yokohama City University Hospital, Yokohama, Japan; ⁴⁹Department of Human Genetics, Research Institute, National Center for Global Health and Medicine, Tokyo, Japan; ⁵⁰Kuwait Medical Genetic Centre, Ministry of Health, Kuwait; ⁵¹Department of Neurology, Azerbaijan Medical University, Baku, Azerbaijan; ⁵²MediClub Hospital, Baku, Azerbaijan; ⁵³Department of Anatomy and Cell Biology, College of Medicine, Alfaisal University, Riyadh, Saudi Arabia; ⁵⁴Department of Neurosciences, University of California San Diego, San Diego, CA; ⁵⁵Rady Children's Institute for Genomic Medicine, San Diego, CA; ⁵⁶GeneDx, Gaithersburg, MD; ⁵⁷Functional Neurosurgery Research

Center, Shohada Tajrish Comprehensive Neurosurgical Center of Excellence, Shahid Beheshti University of Medical Sciences, Tehran, Iran; ⁵⁸Department of Biophysics, Faculty of Biological Sciences, Tarbiat Modares University, Tehran, Iran; ⁵⁹Human Genome Sequencing Center, Baylor College of Medicine, Houston, TX; ⁶⁰Department of Pediatrics, Baylor College of Medicine, Houston, TX

Web Resources

EMBL-EBI. AlphaFold Protein Structure Database. Accessed April 1, 2022. <https://alphafold.ebi.ac.uk>

University of Washington, Hudson-Alpha Institute for Biotechnology, and Berlin Institute of Health. Combined Annotation Dependent Depletion (CADD). Accessed April 1, 2022. <https://cadd.gs.washington.edu/snv>

National Center for Biotechnology Information. dbSNP. Accessed April 1, 2022. <http://www.ncbi.nlm.nih.gov/snp>

Broad Institute of MIT and Harvard. Genome Aggregation Database (gnomAD). Accessed April 1, 2022. <http://gnomad.broadinstitute.org/>

QIAGEN Inc. Human Gene Mutation Database (HGMD) professional 2022.2 Accessed April 1, 2022. <http://portal.biobase-international.com/hgmd>

Berlin Institute of Health. MutationTaster. Accessed April 1, 2022. <http://www.mutationtaster.org/>

Johns Hopkins University. Online Mendelian Inheritance in Man (OMIM). Accessed April 1, 2022. <https://www.omim.org/>

Brigham and Woman's Hospital, Harvard Medical School. PolyPhen-2. Accessed April 1, 2022. <http://genetics.bwh.harvard.edu/pph2/>

Protein Model DataBase. Accessed April 1, 2022. <http://srv00.recas.ba.infn.it/PMDB/>

Bioinformatics Institute. Sorting Intolerant From Tolerant (SIFT). Accessed April 1, 2022. <http://sift.jcvi.org>

Bioparadigms. SLC TABLES. Accessed April 1, 2022. <http://slc.bioparadigms.org/>

Behavioural Phenomics Lab. Tierpsy. Accessed April 1, 2022. <https://tierpsy.com/code>

University of California Santa Cruz. UCSC Genome Browser. Accessed April 1, 2022. <http://genome.ucsc.edu/>

References

- Ng J, Papandreou A, Heales SJ, Kurian MA. Monoamine neurotransmitter disorders—clinical advances and future perspectives. *Nat Rev Neurol*. 2015;11(10):567-584. <http://doi.org/10.1038/nrneurol.2015.172>
- Blackstone C. Infantile parkinsonism-dystonia: a dopamine “transportopathy”. *J Clin Invest*. 2009;119(6):1455-1458. <http://doi.org/10.1172/jci39632>
- Kurian MA, Gissen P, Smith M, Heales S Jr, Clayton PT. The monoamine neurotransmitter disorders: an expanding range of neurological syndromes. *Lancet Neurol*. 2011;10(8):721-733. [http://doi.org/10.1016/S1474-4422\(11\)70141-7](http://doi.org/10.1016/S1474-4422(11)70141-7)

4. Kurian MA, Zhen J, Cheng SY, et al. Homozygous loss-of-function mutations in the gene encoding the dopamine transporter are associated with infantile parkinsonism-dystonia. *J Clin Invest*. 2009;119(6):1595-1603. <http://doi.org/10.1172/JCI39060>
5. Kurian MA. *SLC6A3*-related dopamine transporter deficiency syndrome. In: Adam MP, Mirzaa GM, Pagon RA, et al, eds. *GeneReviews [Internet]*. University of Washington, Seattle; 1993-2022.
6. Fon EA, Pothos EN, Sun BC, Killeen N, Sulzer D, Edwards RH. Vesicular transport regulates monoamine storage and release but is not essential for amphetamine action. *Neuron*. 1997;19(6):1271-1283. [http://doi.org/10.1016/s0896-6273\(00\)80418-3](http://doi.org/10.1016/s0896-6273(00)80418-3)
7. Rilstone JJ, Alkhater RA, Minassian BA. Brain dopamine-serotonin vesicular transport disease and its treatment. *N Engl J Med*. 2013;368(6):543-550. <http://doi.org/10.1056/NEJMoa1207281>
8. Takahashi N, Miner LL, Sora I, et al. VMAT2 knockout mice: heterozygotes display reduced amphetamine-conditioned reward, enhanced amphetamine locomotion, and enhanced MPTP toxicity. *Proc Natl Acad Sci U S A*. 1997;94(18):9938-9943. <http://doi.org/10.1073/pnas.94.18.9938>
9. Jacobsen JC, Wilson C, Cunningham V, et al. Brain dopamine-serotonin vesicular transport disease presenting as a severe infantile hypotonic parkinsonian disorder. *J Inher Metab Dis*. 2016;39(2):305-308. <http://doi.org/10.1007/s10545-015-9897-6>
10. Zhai H, Zheng Y, He Y, et al. A case report of infantile parkinsonism-dystonia-2 caused by homozygous mutation in the *SLC18A2* gene. *Int J Neurosci*. 2021;1-4. <http://doi.org/10.1080/00207454.2021.1938036>
11. Rath M, Korenke GC, Najm J, et al. Exome sequencing results in identification and treatment of brain dopamine-serotonin vesicular transport disease. *J Neurol Sci*. 2017;379:296-297. <http://doi.org/10.1016/j.jns.2017.06.034>
12. Padmakumar M, Jaeken J, Ramaekers V, et al. A novel missense variant in *SLC18A2* causes recessive brain monoamine vesicular transport disease and absent serotonin in platelets. *JIMD Rep*. 2019;47(1):9-16. <http://doi.org/10.1002/jimd.1.2030>
13. Ziats MN, Ahmad A, Bernat JA, et al. Genotype-phenotype analysis of 523 patients by genetics evaluation and clinical exome sequencing. *Pediatr Res*. 2020;87(4):735-739. <http://doi.org/10.1038/s41390-019-0611-5>
14. Patel N, Khan AO, Alsahli S, et al. Genetic investigation of 93 families with microphthalmia or posterior microphthalmos. *Clin Genet*. 2018;93(6):1210-1222. <http://doi.org/10.1111/cge.13239>
15. Sobreira N, Schiettecatte F, Valle D, Hamosh A. GeneMatcher: a matching tool for connecting investigators with an interest in the same gene. *Hum Mutat*. 2015;36(10):928-930. <http://doi.org/10.1002/humu.22844>
16. Karczewski KJ, Francioli LC, Tiao G, et al. The mutational constraint spectrum quantified from variation in 141,456 humans. *Nature*. 2020;581(7809):434-443. Published correction appears in *Nature*. 2021;590(7846):E53. Published correction appears in *Nature*. 2021;597(7874):E3-E4. <https://doi.org/10.1038/s41586-020-2308-7>
17. Bycroft C, Freeman C, Petkova D, et al. The UK Biobank resource with deep phenotyping and genomic data. *Nature*. 2018;562(7726):203-209. <http://doi.org/10.1038/s41586-018-0579-z>
18. Castrignanò T, De Meo PD, Cozzetto D, Talamo IG, Tramontano A. The PMDB Protein Model Database. *Nucleic Acids Res*. 2006;34(Database issue):D306-D309. <http://doi.org/10.1093/nar/gkj105>
19. Tnyasuvunakool K, Adler J, Wu Z, et al. Highly accurate protein structure prediction for the human proteome. *Nature*. 2021;596(7873):590-596. <http://doi.org/10.1038/s41586-021-03828-1>
20. Iyer S, Sam FS, DiPrimio N, et al. Repurposing the aldose reductase inhibitor and diabetic neuropathy drug epalrestat for the congenital disorder of glycosylation PMM2-CDG. *Dis Model Mech*. 2019;12(11):dmm040584. <http://doi.org/10.1242/dmm.040584>
21. Patten SA, Aggad D, Martínez J, et al. Neuroleptics as therapeutic compounds stabilizing neuromuscular transmission in amyotrophic lateral sclerosis. *JCI Insight*. 2017;2(22):e97152. <http://doi.org/10.1172/jci.insight.97152>
22. Sato DX, Kawata M. Positive and balancing selection on *SLC18A1* gene associated with psychiatric disorders and human-unique personality traits. *Evol Lett*. 2018;2(5):499-510. <http://doi.org/10.1002/evl3.81>
23. Stiermagle T. Maintenance of *C elegans*. WormBook: The Online Review of *C. elegans* Biology [Internet]. WormBook; 2005-2018. <https://www.ncbi.nlm.nih.gov/books/NBK19649/>
24. Barlow IL, Feriani L, Minga E, et al. Megapixel camera arrays enable high-resolution animal tracking in multiwell plates. *Commun Biol*. 2022;5(1):253. <http://doi.org/10.1038/s42003-022-03206-1>
25. Javer A, Currie M, Lee CW, et al. An open-source platform for analyzing and sharing worm-behavior data. *Nat Methods*. 2018;15(9):645-646. <http://doi.org/10.1038/s41592-018-0112-1>
26. Javer A, Ripoll-Sánchez L, Brown AEX. Powerful and interpretable behavioural features for quantitative phenotyping of *Caenorhabditis elegans*. *Philos Trans R Soc Lond B Biol Sci*. 2018;373(1758):20170375. <http://doi.org/10.1098/rstb.2017.0375>
27. Benjamini Y, Drai D, Elmer G, Kafkafi N, Golani I. Controlling the false discovery rate in behavior genetics research. *Behav Brain Res*. 2001;125(1-2):279-284. [http://doi.org/10.1016/s0166-4328\(01\)00297-2](http://doi.org/10.1016/s0166-4328(01)00297-2)
28. Paine I, Posey JE, Grochowski CM, et al. Paralog studies augment gene discovery: DDX and DHX genes. *Am J Hum Genet*. 2019;105(2):302-316. <http://doi.org/10.1016/j.ajhg.2019.06.001>
29. Ng J, Heales SJ, Kurian MA. Clinical features and pharmacotherapy of childhood monoamine neurotransmitter disorders. *Paediatr Drugs*. 2014;16(4):275-291. <http://doi.org/10.1007/s40272-014-0079-z>
30. Yaffe D, Radestock S, Shuster Y, Forrest LR, Schuldiner S. Identification of molecular hinge points mediating alternating access in the vesicular monoamine transporter VMAT2. *Proc Natl Acad Sci U S A*. 2013;110(15):E1332-E1341. <http://doi.org/10.1073/pnas.1220497110>
31. Yaffe D, Vergara-Jaque A, Forrest LR, Schuldiner S. Emulating proton-induced conformational changes in the vesicular monoamine transporter VMAT2 by mutagenesis. *Proc Natl Acad Sci U S A*. 2016;113(47):E7390-E7398. <http://doi.org/10.1073/pnas.1605162113>
32. Yaffe D, Forrest LR, Schuldiner S. The ins and outs of vesicular monoamine transporters. *J Gen Physiol*. 2018;150(5):671-682. <http://doi.org/10.1085/jgp.201711980>
33. Ugolev Y, Segal T, Yaffe D, Gros Y, Schuldiner S. Identification of conformationally sensitive residues essential for inhibition of vesicular monoamine transport by the noncompetitive inhibitor tetrabenazine. *J Biol Chem*. 2013;288(45):32160-32171. <http://doi.org/10.1074/jbc.M113.502971>
34. Duerr JS, Frisby DL, Gaskin J, et al. The *cat-1* gene of *Caenorhabditis elegans* encodes a vesicular monoamine transporter required for specific monoamine-dependent behaviors. *J Neurosci*. 1999;19(1):72-84. <http://doi.org/10.1523/JNEUROSCI.19-01-00072.1999>
35. Burns AR, Wallace IM, Wildenhain J, et al. A predictive model for drug bioaccumulation and bioactivity in *Caenorhabditis elegans*. *Nat Chem Biol*. 2010;6(7):549-557. <http://doi.org/10.1038/nchembio.380>
36. Wassenberg T, Molero-Luis M, Jeltsch K, et al. Consensus guideline for the diagnosis and treatment of aromatic L-amino acid decarboxylase (AADC) deficiency. *Orphanet J Rare Dis*. 2017;12(1):12. <http://doi.org/10.1186/s13023-016-0522-z>
37. Kurian MA, Li Y, Zhen J, et al. Clinical and molecular characterisation of hereditary dopamine transporter deficiency syndrome: an observational cohort and experimental study. *Lancet Neurol*. 2011;10(1):54-62. [http://doi.org/10.1016/S1474-4422\(10\)70269-6](http://doi.org/10.1016/S1474-4422(10)70269-6)
38. Zhang Y, Zhang Y, Sun K, Meng Z, Chen L. The SLC transporter in nutrient and metabolic sensing, regulation, and drug development. *J Mol Cell Biol*. 2019;11(1):1-13. <http://doi.org/10.1093/jmcb/mjy052>
39. Duan R, Saadi NW, Grochowski CM, et al. A novel homozygous *SLC13A5* whole-gene deletion generated by Alu/Alu-mediated rearrangement in an Iraqi family with epileptic encephalopathy. *Am J Med Genet A*. 2021;185(7):1972-1980. <http://doi.org/10.1002/ajmg.a.62192>
40. Marafi D, Fatih JM, Kaiyrzhanov R, et al. Biallelic variants in *SLC38A3* encoding a glutamine transporter cause epileptic encephalopathy. *Brain*. 2022;145(3):909-924. <http://doi.org/10.1093/brain/awab369>

-
41. Saitsu H, Watanabe M, Akita T, et al. Impaired neuronal KCC2 function by biallelic *SLC12A5* mutations in migrating focal seizures and severe developmental delay. *Sci Rep*. 2016;6:30072. <http://doi.org/10.1038/srep30072>
42. Hu C, Tao L, Cao X, Chen L. The solute carrier transporters and the brain: physiological and pharmacological implications. *Asian J Pharm Sci*. 2020;15(2):131-144. <http://doi.org/10.1016/j.ajps.2019.09.002>